NTNU
Det skapende universitet

Transporterer atmosfæriske bølger polarlysprodusert NO ned til den midtre atmosfæren

Andreas Amundsen

MSc in Physics
Innlevert: mai 2016
Hovedveileder: Patrick Joseph Espy, IFY

Norges teknisk-naturvitenskapelige universitet
Institutt for fysikk

Acknowledgments

I would like to sincerely thank my supervisor Patrick Joseph Espy for his guidance and patience. He was always available whenever I needed help and advice.

I must also thank Nora Kleinknecht for her assistance with Matlab coding and advice with analyzing data.

At last I need to thank my close friends at Programvareverkstedet for helping me code both in Matlab and LaTeX.

Summary

This study seeks to examine possible origins of nitric oxide (NO) in the middle atmosphere at altitudes between 60 and 80 kilometers. Three distinct hypotheses regarding the origin of mesospheric NO were examined; Local in-situ production from medium energetic particle precipitation (MEP), downward transport facilitated by atmospheric tides and the possibility of auroral activity influencing downward transport. Data from 2008 pertaining to wind speeds, particle precipitation, auroral activity and NO levels were analyzed and cross-correlated to discern possible relationships.

A weak correlation between energetic particle precipitation and NO was identified four to five days after the precipitation events, although this was judged to be incidental due to the delay being inconsistent with the theory of NO production. A moderate correlation between atmospheric tides with wavelengths of 24 hours and increased mesospheric NO was identified after a delay of eight to nine days. However the total atmospheric tide displayed a moderate degree of anti-correlation, implying that the tides may have a small or even detrimental effect on NO transport. The effects on auroral activity on the transport did not seem significant.

Based on these results and the comparably small sample of usable data, this study recommends closer examination of the relationship between atmospheric waves and nitric oxide concentration in the middle atmosphere. The effects of horizontal transport is also a factor which might merit examination.

Hensikten med denne studien var å undersøke potensielle mekanismer bak observerte nivåer av NO-gass i mesosfæren på høyder mellom 60 og 80 kilometer. Tre hypoteser ble formulert og undersøkt i denne sammenheng. Lokal produksjon av NO gjennom energetisk partikkelstråling fra solvind, transport av NO gjennom atmosfæriske bølger og muligheten for at auroraaktivitet modulerer atmosfæriske bølgers evne til å transportere NO. Data fra 2008 angående vindhastigheter, NO-konsentrasjoner, auroraaktivitet og partikkelstråling fra solvind ble bearbeidet og analysert. Data over konsentrasjoner av NO ble korrelert med vind, partikkelstråling og polarlysaktivitet i henhold til forutsigelser basert på de tre hypotesene.

En svak korrelasjon mellom mellom partikkelstråling og lokal produksjon av NO ble observert fem dager etter strålingsaktiviteten, men dette ble vurdert som urelatert fordi en slik forsinkelse ikke stemte overens med teorien om NO-syntese. En moderat korrelasjon mellom atmosfæriske bølger med bølgelengder på 24 timer og endringer i NO-konsentrasjon ble observert åtte til ni dager etter bølgene. Denne forsinkelsen var ikke problematisk i forhold til gjennomsnittelig levetid av NO i de relevante høydene og lengdegradene. Resultatene antydet ikke at polarlys hadde en stor effekt på de atmosfæriske bølgene i henhold til transport av NO.

Basert på disse resultatene og den relativt begrensede mengden av brukbare data som ble analysert, så foreslår denne studien ytterligere undersøkelser av sammenhengen mellom atmosfæriske bølger og NO-konsentrasjoner i mellomatmosfæren.

Table of Contents

Chapter 1

Introduction

Nitric oxide (NO) is part of the highly reactive group of atmospheric gases known as ”NOx gases”. It is an important part of atmospheric chemistry, mainly due to its properties as a strong catalyst for destroying ozone (O_3). Ozone is an important part of the atmosphere's temperature regulation by heating the stratosphere, as well as a protective layer against UV radiation which is harmful for most lifeforms. This makes it relevant to examine the subject of synthesis and transport of NO throughout the atmosphere. The aurora is a well known source of NO gas at altitudes above 90 kilometers, but less is known about the mechanisms behind the presence of NO at altitudes between 60 and 80 kilometers. At these altitudes NO has a far longer lifetime compared to above 90 kilometers and further downward transport is therefore more likely. NO which reach the stratosphere will have a very long lifetime, which would allow even small amounts to dissociate large amounts of ozone.[1]

One plausible mechanism behind mesospheric NO is local production in the middle atmosphere caused by precipitation of energetic particles. This would imply an increased concentration of nitric oxide following high precipitation activity, and is something which may be observed using available data. Another possible explanation would be downward transport of aurora produced NO facilitated by large-scale perturbations of the air column known as atmospheric tides. This would likewise imply increased NO concentration after strong tides, although a certain delay could be allowed for. There is also a need to consider whether or not such downward transport could be modulated by auroral activity, the analogy being that little NO would be transported downwards if there are small amounts available for transport at the time the tides occurs.

A large body of data regarding all involved phenomena was required in order to test the hypotheses. These included wind speeds, auroral activity, energetic precipitation measurements and NO-concentrations. The data would also need to coincide in terms of geographical coordinates and span similar time periods. Based on these criteria, the area above the Norwegian research station Troll (-72.0113° S,2.535 ° E) and the year 2008 was chosen. Troll research station is situated within the polar vortex, a large-scale weather system each winter which causes downward transport from the upper atmosphere, and was therefore an ideal location to test potential correlation between atmospheric tides and NO-concentrations in the middle atmosphere.[2]

Chapter 2

Theory

2.1 Hypotheses

In order for any kind of data analysis to be meaningful, it is necessary to have a hypothesis to provide a framework for interpretation. This study formulates three hypotheses in order to explain the amount of nitric oxide (NO) present in the middle atmosphere, and testing these was a matter of comparing predicted results with actual data samples.

The first hypothesis is that the NO is being produced locally at altitudes between 60 and 80 kilometers. This study considers medium energetic precipitation (MEP) to be a likely source of such production, and is therefore selected for further analysis. This hypothesis predicts that there exists a positive correlation between NO-concentration and MEP activity. Testing this prediction requires a correlation analysis between energetic precipitation activity and NO-concentration over the same time period.

The second hypothesis is that NO produced in the thermosphere (above 90 km) is transported downwards into the mesosphere (60-80 km), and that this is facilitated by atmospheric tides. This hypothesis predict a correlation between these phenomena, meaning increased levels of NO is expected after strong atmospheric tides.

The third hypothesis is a variant of the second. Instead of assuming a constant pool of NO available for transport, it postulates that the amount of NO transported downwards by the atmospheric tides is modulated by auroral activity. The aurora is a known source of thermospheric NO. The reasoning behind this hypothesis is that if little NO is present at the time of a strong atmospheric tide, there will be little available for downward transport. This hypothesis predicts a correlation between NO levels and atmospheric tides modulated by auroral activity.

2.2 Atmospheric structure

The atmosphere is a layer of gases held in place by the Earth's gravity, consisting mainly of approximately 78 percent N_2 and 21 percent O_2. The remaining gas species are mainly CO_2, water vapor, ozone (O_3) and argon. The atmosphere may be divided into several vertical layers based on properties such as pressure, composition and temperature. Figure 2.1 depicts a general listing of the atmospheric layers at respective altitudes[3].

From the surface up to around 15 km is referred to as the troposphere, which is followed by a brief transitional layer called the tropopause where the temperature starts to increase rather than decrease with height. Above this, the stratosphere ranges from approximately 20 to 42 km. The notable increase temperature in this region is due to the ozone layer, which is heated by ultraviolet radiation from the sun through the synthesis and dissociation of ozone. The stratosphere is bounded by another transitional region called the stratopause, followed by the mesosphere which ranges from 50 to 90 km. The stratosphere and mesosphere together is often referred to as the middle atmosphere. Altitudes above 95 kilometers is referred to as the thermosphere and is a region consisting mostly of ionized gases at very low densities. The aurora generally takes place in the thermosphere. The region between 690 and 100 000 kilometers is referred to as the exosphere, and forms the formal boundary between the atmosphere and interplanetary space.[3]

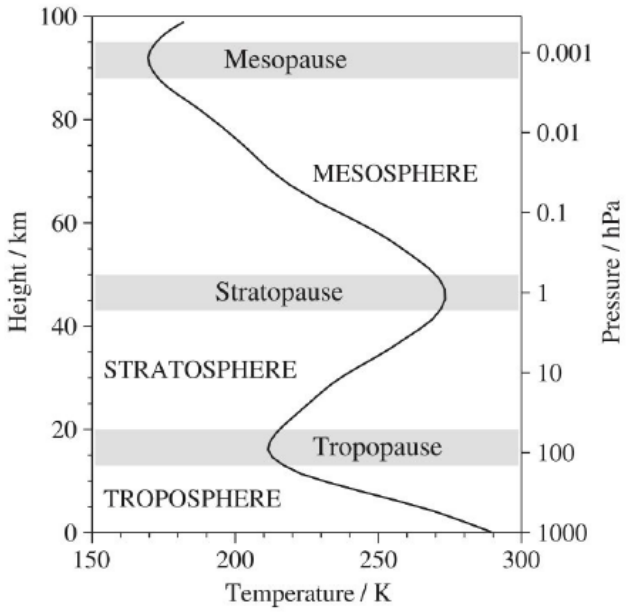

Figure 2.1: The Earth's atmospheric layers, pressure and average temperature with increasing altitude. Figure taken from [3].

The physical properties of the upper atmosphere are usually approximated reasonably well with using the ideal gas law(2.1), which describes the relationship between the pressure, temperature and volume in a given parcel of gas. While the ideal gas law works best for monoatomic gases at

low temperatures, and the atmosphere's temperature varies greatly and contains several diatomic gas species including water vapor, the conditions of the middle and upper atmosphere makes the ideal gas law an acceptable approximation for the purposes of this study, since water vapor makes up less than a few parts per million of the total gas number density. The assumption of adiabatic movement of air parcels is used in order to calculate the number density of gas species, nitric oxide in this case.[3]

$$PV = nk_BT \tag{2.1}$$

Where n is the number of molecules in the gas, k_B is the Boltzmann constant, V is the volume, p is the pressure and T is the temperature in Kelvin.

Volume mixing ratio for a general gas species a is expressed through the equation (2.2).

$$v_a = \frac{[n_a]}{[n_p]} = \frac{V_a}{V} \tag{2.2}$$

Where $[n_a]$ is the number density (molecules/volume) of the gas species a and $[n_p]$ is the total number of particles in the air parcel. V is the volume the gas displaces and V_a is the partial volume of gas species a.

The pressure may also be expressed as (2.3).

$$p = [n_p]k_BT \tag{2.3}$$

The concentration of a general gas species a may therefore be expressed using equation (2.4).

$$[n_a] = \frac{v_a \cdot p}{k_B \cdot T} \tag{2.4}$$

2.3 Atmospheric wave phenomena

Wind is essentially large-scale movement of air driven by pressure gradients in the atmosphere. The expansion and contraction of air following heating and cooling results in pressure differences which will create wind. Daytime heating and nighttime cooling, as well as the increased heating of equatorial regions compared to the polar regions are the main causes. The 23 degree tilt on the planet's rotational axis also creates uneven heating, which results in seasonal effects on the wind systems. The Coriolis force from the Earth's rotation and the moon's tidal forces also effects the wind system. The periodic nature of these factors gives rise to several oscillating phenomena, such as gravity waves, planetary waves and atmospheric tides. [3] For the purposes of this study, atmospheric tides are tested as the likely candidate for downward transport of NO.

2.3.1 Atmospheric tides

Atmospheric tides is a phenomena created by daytime heating and nighttime cooling of the atmosphere. As these are periodic events with a length of 12 hours, the resulting oscillations does also exhibits a periodicity related to this period. As with other physical wave phenomena, the atmospheric tides may be written as a sinusoidal superposition of several tidal components of different periods. Prominent periods of atmospheric tides are 24, 12 and 8 hours, where the 12 and 24-hour components are the strongest [4]. These two components were therefore selected as the main candidates for downward transport of NO.

An oscillation with a period of 48 hours would also be apparent from the atmospheric tide oscillations, although this is a planetary wave and not a tide. These arise as a result of the viscosity of the atmosphere in combination with the Coriolis force.

2.4 Nitric oxide chemistry

Nitric oxide (NO) belongs to the group referred to as NOx. In the upper atmosphere the main NO production occurs when energetic photons or particles interacts with nitrogen molecules and oxygen. There are three main chemical pathways which yields NO^+-ions, all of which will react with oxygen to eventually form neutral NO molecules. Sufficient N_2, O and O_2 is assumed for the purposes of the following chemical reactions.[5]

Equations (2.5) and (2.6) describes how N_2 reacts with energetic electrons or photons ($h\upsilon$), forming positive NO-ions and excess nitrogen atoms.

$$N_2 + e^- \text{ or } h\upsilon \longleftrightarrow N_2^+ + e^- \tag{2.5}$$

$$N_2^+ + O \longleftrightarrow NO^+ + N \tag{2.6}$$

The second chemical pathway described in equation (2.7) and (2.8) is oxygen atoms reacting with energetic electrons or photons, eventually resulting in NO^+ ions and excess nitrogen atoms.

$$O + e^- \text{ or } h\upsilon \longleftrightarrow O^+ \tag{2.7}$$

$$O^+ + N_2 \longleftrightarrow NO^+ + N \tag{2.8}$$

The third pathway is given by equations (2.9) and (2.10), where O_2 molecules interacts with electrons or photons to form a charged O_2 molecule, which will interact with neutral NO to form NO^+ and O_2 molecules.

$$O_2 + e^- \text{ or } h\upsilon \longleftrightarrow O_2^+ \tag{2.9}$$

$$O_2 + NO \text{ or } h\upsilon \longleftrightarrow NO^+ + O_2 \tag{2.10}$$

The positive NO ions created by these reactions may then react with electrons as described in equation (2.11), forming excited nitrogen atoms. The excited nitrogen has a 85% chance of having a ^{2}D electron shell configuration, and a 15% chance of a ^{4}S electron shell configuration. Both will result in neutral NO molecules when reacting with O_2 as described in (2.12), albeit the N(^{2}D) configuration has a much faster reaction rate.[2]

$$NO^+ + e^- \longleftrightarrow N(^4S) \text{ or } N(^2D) \tag{2.11}$$

$$O_2 + N(^4S) \text{ or } N(^2D) \longleftrightarrow NO \tag{2.12}$$

The average lifetime of NO at heights of 80 to 120 kilometers varies between 1 and 5 days depending on latitude. It is 2.5 days in the tropics while being closer to 5 days in the auroral region. The latter estimate is more relevant due to data being taken from latitudes around -72°S within the southern auroral oval. The main factor in NO-destruction is photo dissociation from 191 nm photons, which is a part of the ultraviolet spectrum. During polar nights in winter when little to no sunlight hits the atmosphere, NO lifetime is very long and similarly at heights below 40 km due to the protection offered by the denser atmosphere. For the purposes of this study, the rate of ionization is assumed to be 35 eV on average per ion-electron pair, meaning an ionization occurs per 35 eV which is deposited in a given area.[2]

Equation (2.13) to (2.14) describes NO's role as a catalyst for ozone dissociation, which combined with its extensive longevity at altitudes congruent with the ozone layer makes it a potent ozone depleting agent. A catalyst is defined as a substance facilitating a chemical reaction while either regenerating itself or not being destroyed in said reaction. This allows the catalyzing substance to continue mediating reactions and recycle itself as long as the conditions are right.

$$NO + O_3 \longleftrightarrow NO_2 + O_2 \tag{2.13}$$

$$NO_2 + O \longleftrightarrow NO + O_2 \tag{2.14}$$

2.5 Energetic Particle Precipitation (EPP)

Solar wind contains large amounts of highly energetic and charged particles, photons as well as strong electric and magnetic fields. When these clouds of plasma approaches the Earth, the magnetic fields generated by the charged particles interact with the Earth's magnetic field, causing charged particles to deflect from their trajectories and follow the field lines pointing away from the north and south poles. The energetic particles from the solar wind will then strike atmospheric gases and cause particle excitation and ionization events, giving rise to electron emission and numerous other chemical reactions. Figure 2.2 provides a simplified illustration of this phenomena.[2]

The aurora is one of the directly visible effects of solar wind hitting the Earth, and it generally occurs throughout the thermosphere at latitudes between 10 and 20 degrees away from the geomagnetic poles, which move from year to year. The band of latitudes and longitudes the aurora commonly occurs at is referred to as the auroral oval. Following particularly strong solar particle precipitation the aurora might be visible at far lower latitudes.

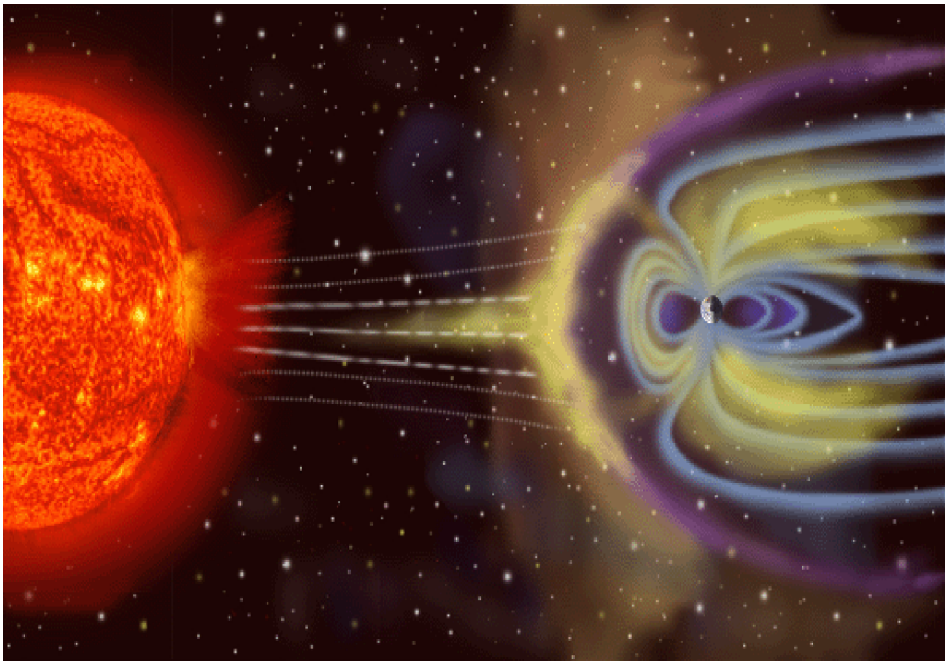

Figure 2.2: The Earth's magnetic field is regularly struck by solar winds, which causes and influx of energetic particles.[2]

Refer to figure **Fig. 2.2**

The energy of the incoming electrons is also an important point, as particles with more energy penetrate further into the atmosphere. The energies which penetrate to altitudes from 60 to 80 kilometers are predominantly between 100 keV and 1 MeV[5] as seen in Figure 2.3. Particle precipitation of energies between 50 keV and 1 MeV is referred to as medium energy precipitation (MEP). Between altitudes of 90 to 120 kilometers the precipitation energies generally range between 1 to 20 keV, which is referred to as energic electron precipitation (EEP). The energies required to induce NO

production is 35 eV, meaning that energetic particles will deposit on average 35 eV per ionization until they thermalize with their surroundings.[2][5]

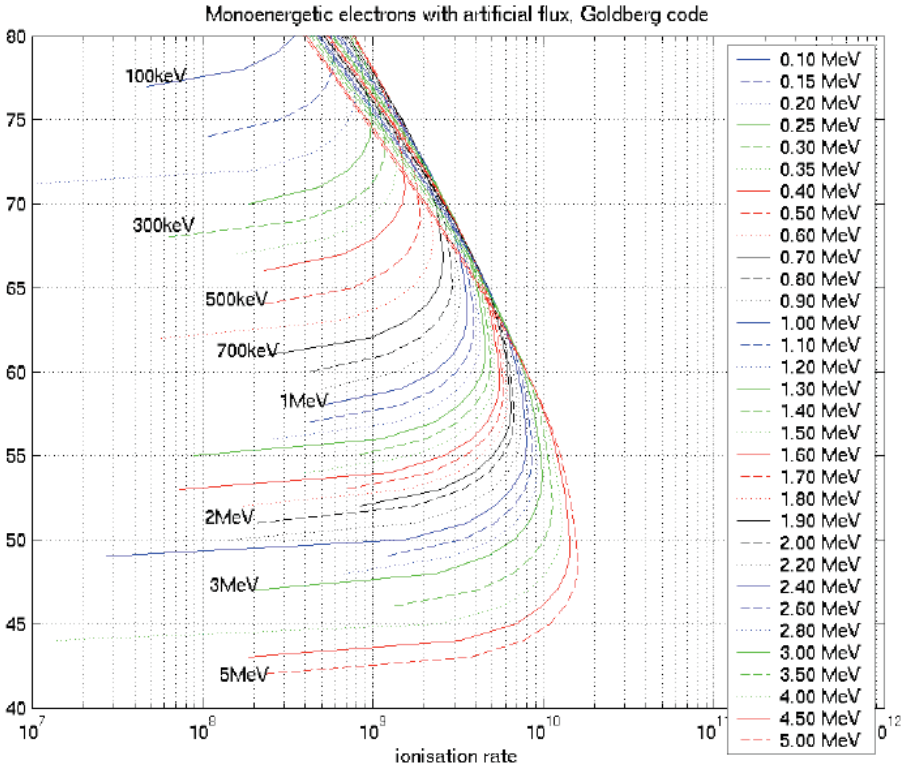

Figure 2.3: The ionization rates per altitude of electron precipitation with energies ranging from 100 keV to 5 MeV. At altitudes from 80 km to 60 km, the majority of ionization is performed by electrons of energies between 100 keV and 1 MeV. Figure taken from lecture by E. Turunen.[5]

2.6 Auroral Electrojet

The auroral electrojet (AE) is a current of charged particles flowing at altitudes from 100 to 150 kilometers, usually on latitudes between 60 and 70 degrees inside the so-called auroral oval. It displays both an eastward and a westward component and energetic particle precipitation is the main driving force behind the auroral electrojet, as this phenomena is directly coupled to the aurora. This makes the AE suitable as an approximation of auroral activity. The World Data Center for Geomagnetism in Kyoto had gathered and compiled data from several research stations in the northern hemisphere to create an index of AE values from 1957 to the present.[6]

Measuring the activity of the auroral electrojet is done by measuring the Earth's geomagnetic field on the surface. The current of charged particles moving in the auroral region induces significant magnetic fields which may be measured at ground based observatories. These field changes may be in the order of hundreds of nanotesla (nT), and correlate both to an eastward and westward component. The average of these components is referred to as the AE index.

The fact that the data was acquired from the northern hemisphere is an important detail. This requires some assumptions to be made regarding the symmetry of northern and southern auroral activity. In order to proceed with the analysis the assumption is made that the auroral activity of the northern and the southern hemisphere is symmetrical to the extent of displaying increased activity within the same day as the precipitation from solar wind occurs. For this assumption to hold, a significant correlation over the course of a day between the AE-index and particle precipitation activity needs to be observed.

Chapter 3

Data and analysis

3.1 NO data

3.1.1 VMR

The Norwegian research station Troll in Antarctica (-72.0113° S,2.535 ° E) provided daily nitric oxide measurements spanning 2008 and 2009[7]. The measurements were taken above the research station using a heterodyne radiometer. This instrument consists of a cryogenically cooled radiometer coupled to a spectrometer observing the relevant parts of the microwave spectrum, specifically a frequency of 250.796 GHz in the case of NO.[1]

This data had already been processed using temperature and pressure measurements to give the volume mixing ratio given in parts per million, meaning that it was only necessary to extract and sum over the desired altitudes of 60 to 80 kilometers. This was done in order to obtain the data needed to calculate the NO-concentration. The estimated VMR-values could be negative due to instrument noise, but these were interpreted to represent no measured NO and set to 0. Numerous missing entries during the first 50 days of 2008 limited the data usable for the correlation analysis.

3.1.2 Concentration

The data set containing the daily volume mixing ratio in parts per million, listed in altitude intervals of one kilometer, was . A supplementary file containing temperatures and pressure was also included for the purposes of finding the concentration of NO. The approximation of dry air was chosen for the purposes of calculation, as the mesosphere contains very few water molecules. The equation relating concentration of a specific gas species in a parcel of air to volume mixing ratio was based on equation (2.4) from the theory section. The concentration on each day for every height were calculated in Matlab and in order to find the column density of NO molecules measured in molecules per cm^2, all entries from 60 to 80 kilometers were integrated. The end result

was finally converted to the proper units and stored for later use.

3.2 Wind data

The wind data was obtained from the South African research station Sanae IV (-71.6728° S, -2.8406° W), a part of the SuperDARN radar network[7]. For the purposes of finding the tidal amplitude, the meridional wind (north-south direction) was used. The data set listed hourly wind speeds as well as numerous other factors, although only data points containing measured data were listed. Note that it only covered up to 01:00 on the 28th of June 2008, thus limiting the overlap with the other data sets significantly.

Due to missing data points not being listed in the data file, the first step was to expand the vector to cover every hour of the year by filling in NaNs (Not a Number) to represent missing measurements. The next step was to exclude unwanted data and the criteria for excluding a window was closely based on a paper by R. Hibbins from 2008[4]. This list of exclusion criteria included wind speeds over 100 m/s, measurements taken from other geographical coordinates and data where the standard deviation of zonal or meridional wind were 0. Windows also needed to span at least 48 hours, and more than 12 missing data points over 48 hours were required. Regular gaps longer than 3 hours on the same hours every day were also removed. In the end less than half the windows were used to generate the tidal fit. The fitting was started 36 hours before 00:00, 1st of January 2008 in order to center the window on a given day, by spanning 36 hours in both direction of the 24 hours of any given day. Note that this would mean an effective loss of two days of measurements at the end of the data set.

When applied to the fitting routine, the data was sectioned into four-day (96 hour) intervals which were shifted by 24 hours until the end of the data set had been reached. These intervals, or "windows", were then fitted using a model consisting of a superposition of four distinct sine functions of varying wavelength as well as the average amplitude A_{mean} for the given window (3.1). The Matlab toolbox curve fitting tool (cftool) was utilized to create the fitting routine, which was then repeated for every 96-hour window.

$$A_{mean} + A_{48}sin(\frac{2\pi t}{48} + \phi_{48}) + A_{24}sin(\frac{2\pi t}{24} + \phi_{24}) + A_{12}sin(\frac{2\pi t}{12} + \phi_{12}) + A_{8}sin(\frac{2\pi t}{8} + \phi_{8}) \quad (3.1)$$

Where A_n is the amplitude of the n-hour tidal component, and ϕ_n is the corresponding phase.

The results of the fitting routine were then stored in a matrix containing The average meridional wind, the 48-hour, 24-hour, 12-hour and 8-hour components as well as their corresponding phases. Each of the amplitudes represented the peak value of the given component of the total atmospheric tide on a given day. The phases represented the point in time during the fitted period the wave reached the peak value. Note that the waves were fitted over four days, and the 24 hours in the center was treated as the day the amplitude occurred. Because the 24 and 12-hour periods were the

strongest[5], these were selected for the correlation analysis. A vector sum of the 24 and 12 hour components was also calculated like depicted in figure 3.1.

The 48 hour was a planetary wave and therefore a mostly horizontal wave not expected to contribute to vertical transport. See the appendix for the correlations of the 48 and 8 hour components.

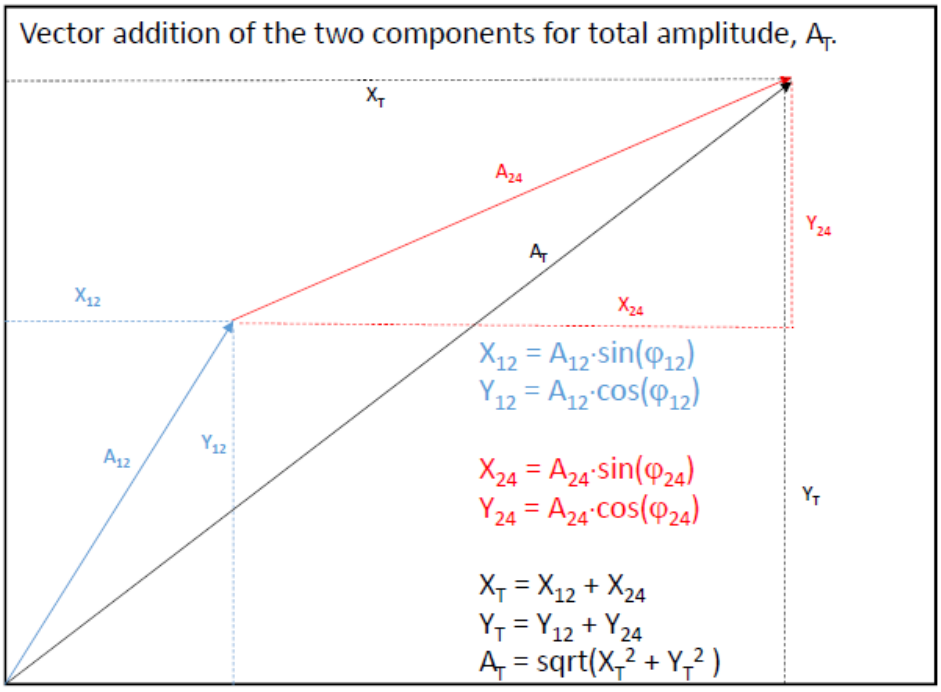

Figure 3.1: Visual reference of the vector sum of the 24 hour and 12 hour amplitude component and their phases.

In order to simulate the effects of the AE-index modulating the tidal amplitudes, a simple vector multiplications of the AE-values and the tidal amplitudes was performed. So the 12 hour, 24 hour and total tidal amplitude at day 1 were multiplied with the AE-index at day 1, creating an estimate of how much NO would be available for downward transport on any given day.

3.3 MEP data

Data for Medium Energetic Particle precipitation during the year 2008 was gathered from the measurements of four satellites from the POES satellite system orbiting the southern hemisphere[8], and it covered the entire year. The data contained a varying number of entries for each day, which were also irregularly spaced in time. As each satellite orbited large parts of the southern hemisphere, it was necessary to remove all data not within the relevant latitudes and longitudes. The area of interest was defined as every entry measured within a five degree "box" of the Troll research station (-72.0113° S,2.535 ° E).

The data set contained energy deposition for each 1 km height-bin for every date, and was given in keV per cm^3 per s ($\frac{keV}{cm^3 s}$). First all measurements containing geographical coordinates outside a 2.5° box around the Troll research station were excluded, then the energy deposition for the relevant altitudes (60 to 80 km) were integrated in order to find the column deposition $\frac{keV}{cm^2 s}$. This was repeated for each of the four satellites and the list of measurements for every date in time were compiled and ordered in time. Due to each day containing a varying number of unevenly spaced measurements, a Simpson's method integration was performed to calculate daily total energy deposition given in $\frac{keV}{cm^2}$. This could finally be converted to an estimated ions per cm^2 by dividing with $35 \cdot 10^{-3}$,based on the assumption of one ionization event occurring per 35 eV of energy entering a given square centimeter.

3.4 AE data

The hourly auroral electrojet index for 2008 was acquired from the World Data Center for Geomagnetism in Kyoto[6]. There was no need to further process the AE-index itself, as the daily averages were already calculated. However, the AE-indices were derived from geomagnetism measurements performed by several ground-based observatories in the northern hemisphere. This was an important as discussed in the theory, due to the other data sets being gathered from the southern hemisphere. Because of this it was necessary to assume that aurora activity was sufficiently symmetrical between both hemispheres for the purposes of this study. A cross-correlation between the MEP-data and the AE-index was performed in order to justify this assumption.

3.5 Cross-correlation analysis

The correlation analysis was performed using a Matlab script which loaded the data concerning all phenomena mentioned above ordered by day of year. The relevant data sets were then processed using the ”xcorr()” function in Matlab and lagged in positive and negative directions to obtain the correlation coefficients for various delays. Due to the data containing one data point per day, the delays were given in days as well. The correlation coefficient between two arbitrary data sets a and b can be expressed as r, which ranges between -1 and 1. A positive coefficient means that an increase in one data set following increase in the other, while negative correlation coefficient would translate to a decrease in one parameter following an increase in the other.

The exact ratio of how related the two data sets are can be expressed as r^2, which is called the coefficient of linear correlation and ranges between 0 and 1. This is a ratio of how much of the variation in data set a can be accounted for by the variation in data set b. For example, a correlation coefficient r of 0.5 would translate to a coefficient of linear correlation r^2=0.25. This quadratic relation means that smaller r values equates to much smaller r^2 values.

Correlation coefficients ranging between 0 and 0.3 are generally considered to denote a weak positive correlation. Coefficients between 0.3 and 0.5 generally denotes a moderate correlation, while coefficients ¡0.6 are considered good correlation. The same thresholds are used for negative correlations coefficients. A value of 0 denotes no correlation, meaning that the data sets does not influence each other at all.

The cross-correlation routine lagged one data set relative to the other set, drawing a graph of correlation coefficients at the respective amounts of positive and negative lag. In this case the lags were measured in days. For the correlations involving nitric oxide concentrations, the NO-data were lagged relative to whatever other data set it was correlated with. So if there for instance were a high r^2 value at a positive lag of 5 days it would mean an increase in the NO values was observed 5 days after the other phenomena occurred. A positive correlation coefficient occurring at negative lag would translate to the NO increasing before the event occurred. While the negative lags were not instrumental to the study, calculating both positive and negative lags was helpful due to repeating phenomena always having both positive and negative lags.

For the hypothesis of local production of NO based on particle precipitation, an instant and positive correlation was predicted. For the wind amplitudes correlated with NO, the first significantly large correlation coefficient would generally be the most interesting due to the lifetime of NO gas. Some delay should be expected due the time it would take to transport NO from altitudes above 90 km to 60-80 km.

Chapter 4

Results and discussion

4.1 NO data

Integrated daily volume mixing ratio in parts per million for 2008 is displayed in Figure 4.1. The number density, or concentration of particles per cm^2, is displayed in Figure 4.2. Note the lack of data points during the first 50 days. This limited the time period usable for the correlation analysis. The cross-correlation was therefore performed from day 50.

The comparably high VMR-values compared to the relatively even level of the number density was rather apparent. This reflects that these two measurements do not measure the same thing. A low volume mixing ratio at high pressure would still constitute a high number density.

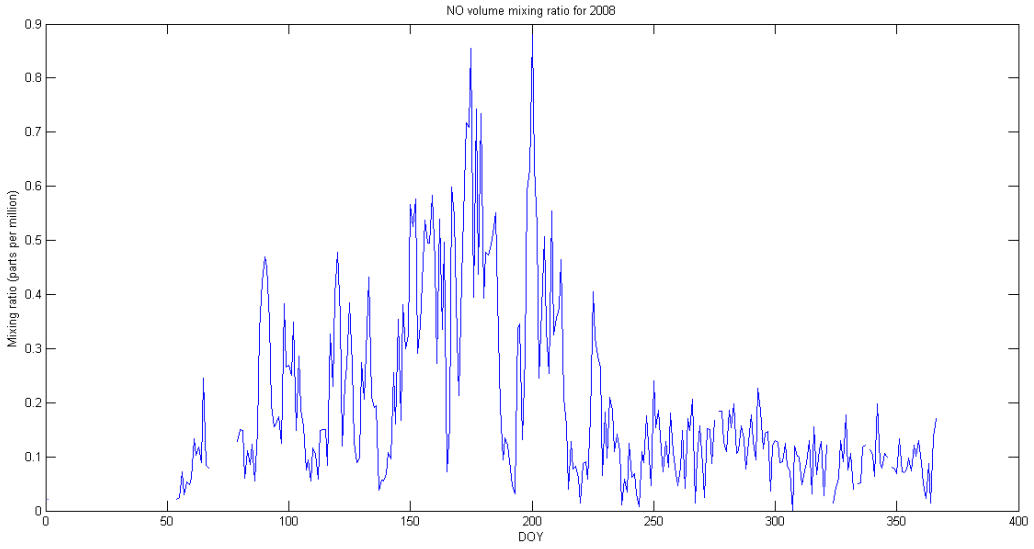

Figure 4.1: NO volume mixing ratio in ppm for 2008, integrated over altitudes from 60 to 80 kilometers.

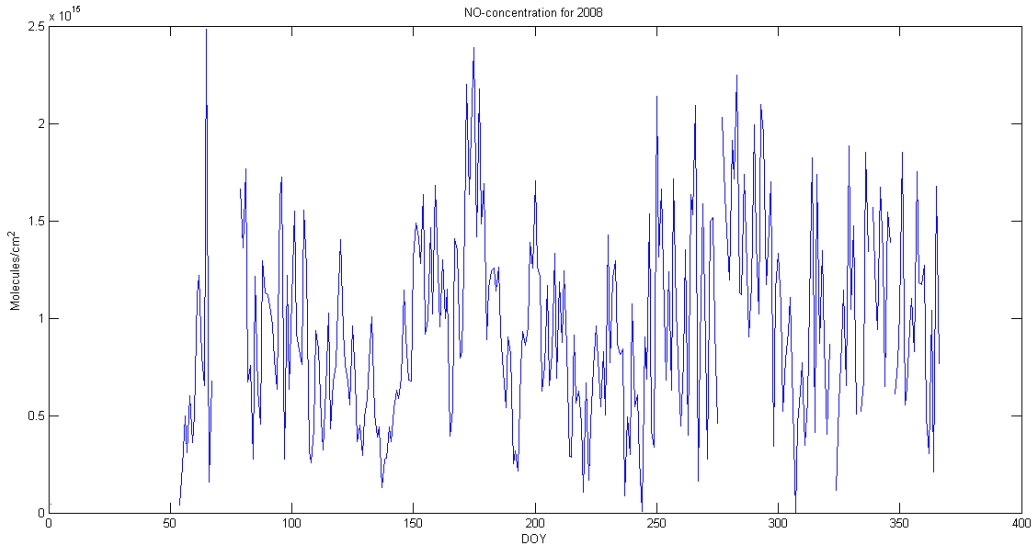

Figure 4.2: NO-concentration in molecules per cm^2 for 2008, integrated over altitudes from 60 to 80 kilometers.

4.2 Wind data

Figure 4.3 depicts the raw data of the meridional wind, meaning the north-south direction, given as hourly wind speeds. Whether the value was listed as positive or negative depended on the direction of the wind relative to the line of sight from the observatory. Visible wave phenomena were clearly occurring and the purpose of the fitting routine was to identify these.

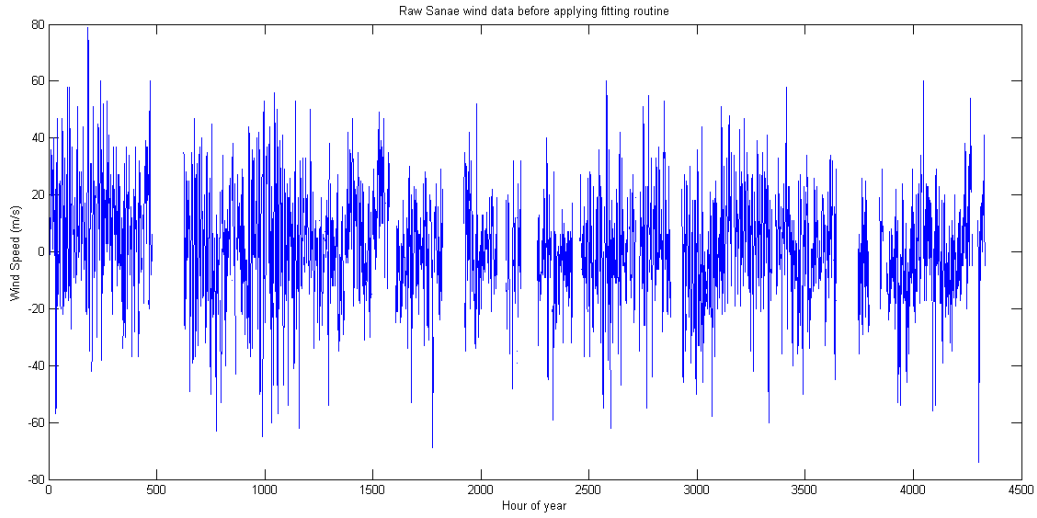

Figure 4.3: The raw, unprocessed meridional wind data from the Sanae research station.

Figure 4.4 displays an example of a individual window being fitted, and Figure 4.6 displays the respective amplitudes of the 24 hour and 12 hour components of each day, as well as their phases. Figure 4.5 displays the vector sum of the 12 and 24 hour components, also known as the total tide. These two tidal components were used for the cross-correlation analysis. The fitted amplitudes ended up rather incoherent due to missing measurements and eliminated outliers, but general trends were still apparent. Note that the data covered up to 01:00 the 28th of June, which combined with the loss of two days due to nature of the 96-hour windows meant that the wind data spanned only 176 days out of 366.

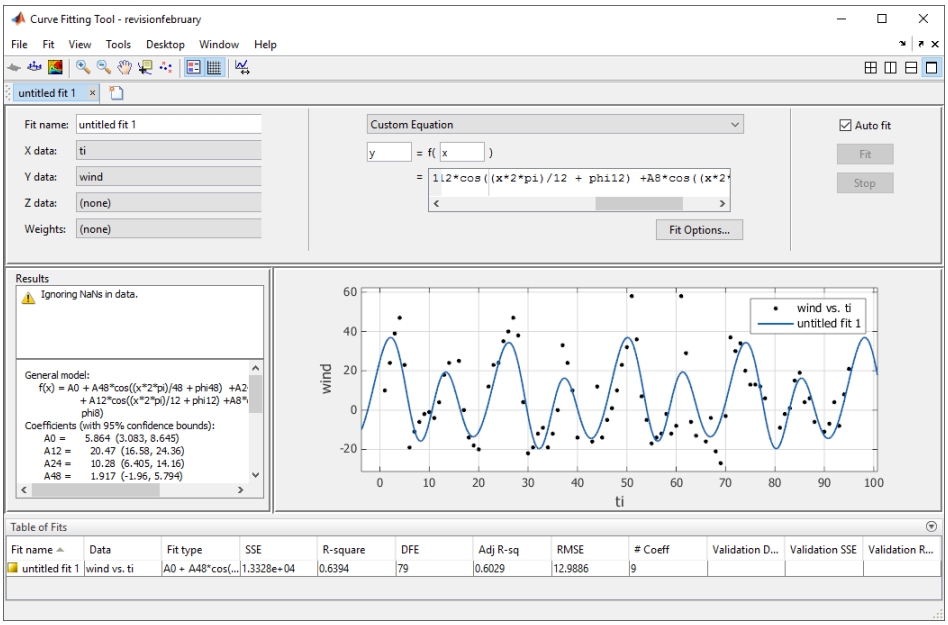

Figure 4.4: Example of fitting using the built-in function cftool in Matlab. The fitting-routine code was generated using this functionality as a template.

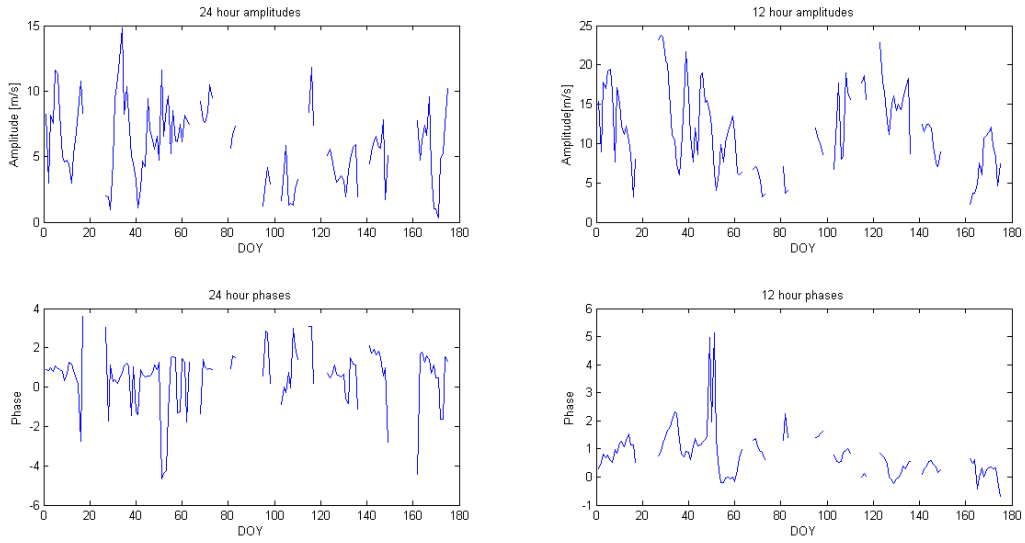

Figure 4.5: Overview of 24 hour tidal amplitudes, 12 hour tidal amplitudes and their respective phases.

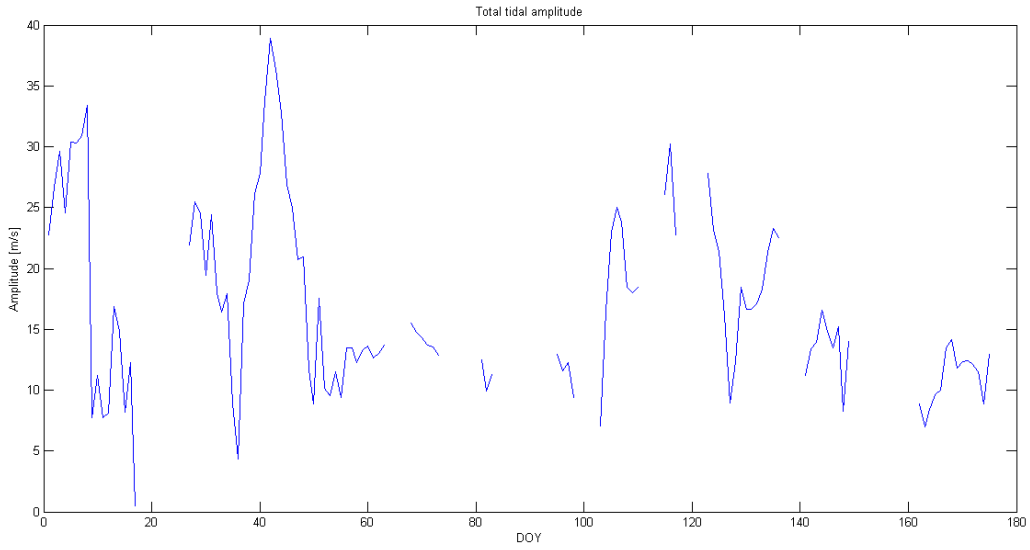

Figure 4.6: The vector sum of the 12 and 24 hour tidal amplitudes, also known as the total tide.

4.3 MEP data

The Medium Energy Precipitation values are depicted in Figure 4.7. Figure 4.8 displays this data as NO^+-ions per square cm, assuming that 35 eV per square centimeter would induce one ionization event. Due to the chemistry discussed in the theory, all NO^+-ions are assumed to end up as neutral NO.

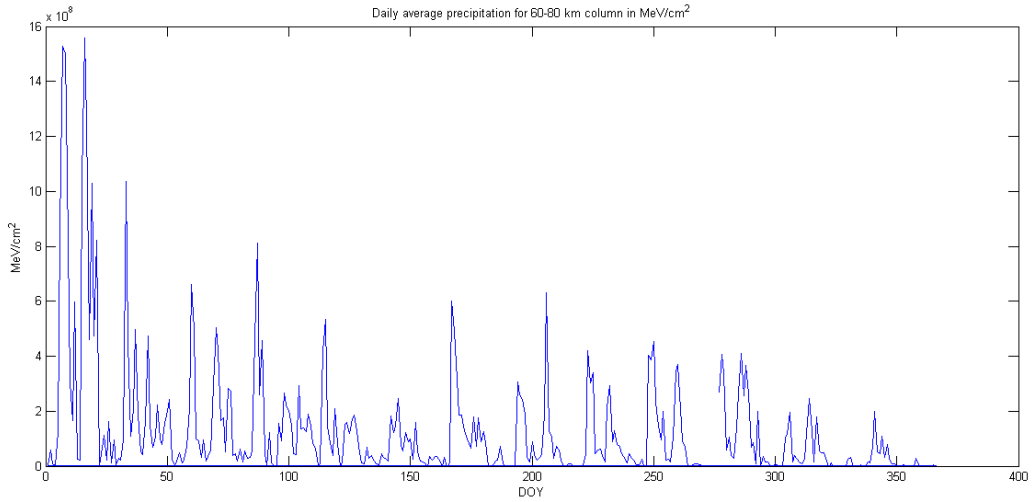

Figure 4.7: Integrated energy precipitation (MEP) between 60 and 80 km, expressed in $\frac{MeV}{cm^2}$.

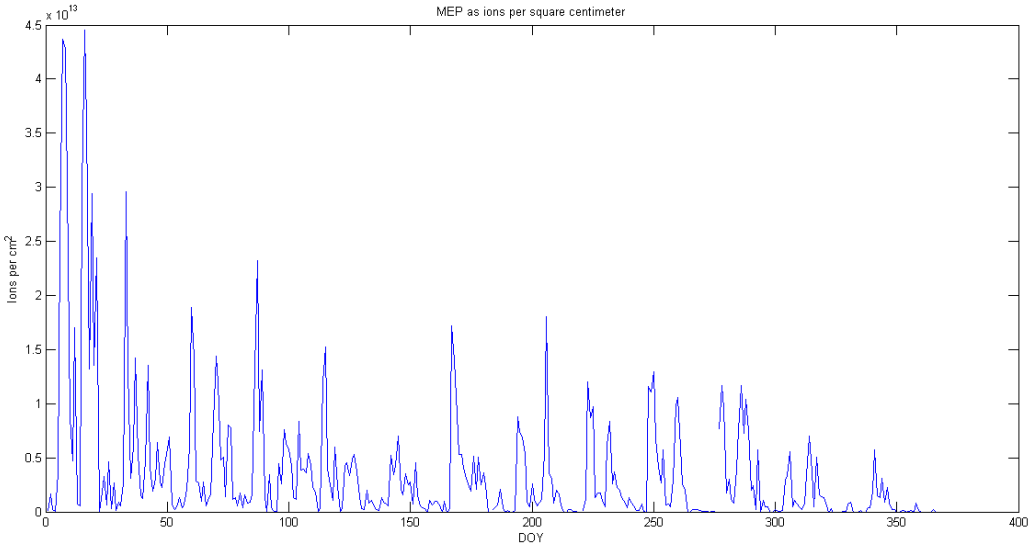

Figure 4.8: MEP converted to estimated number of NO^+-ions per square centimeter.

4.4 AE data

Figure 4.9 depicts the daily mean auroral electrojet index for 2008.

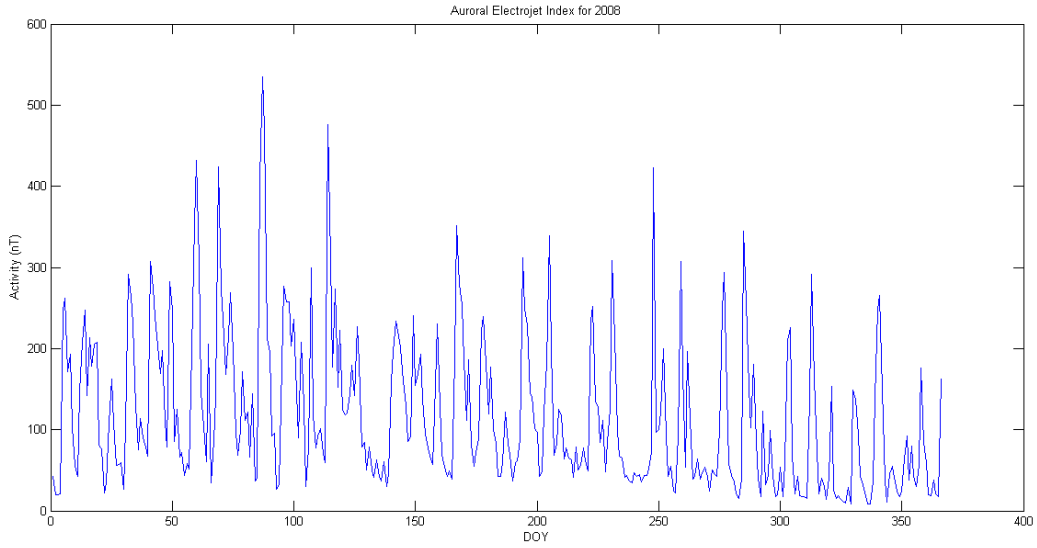

Figure 4.9: Daily mean AE-index for 2008 measured in nanoTesla.

4.4.1 AE-index correlated with MEP

The correlation between the AE and the particle precipitation MEP is depicted in figure 4.10. Note the relatively high correlation of at day 0 and 1, with r^2 values 0.7409 and 0.6688 respectively. This translates to a good correlation according to the theoretical thresholds of correlation coefficients. This gives r value of 0.5489 for day 0, meaning that 54.89 percent of the variation in the AE could be accounted for by the MEP-activity occurring the same day. Given these numbers, the assumption of the AE-index being related to MEP-activity

The correlations also displays a 27 day cycle, which is This means that the AE-modulated tides are expected to display a 27 day cycle as well.

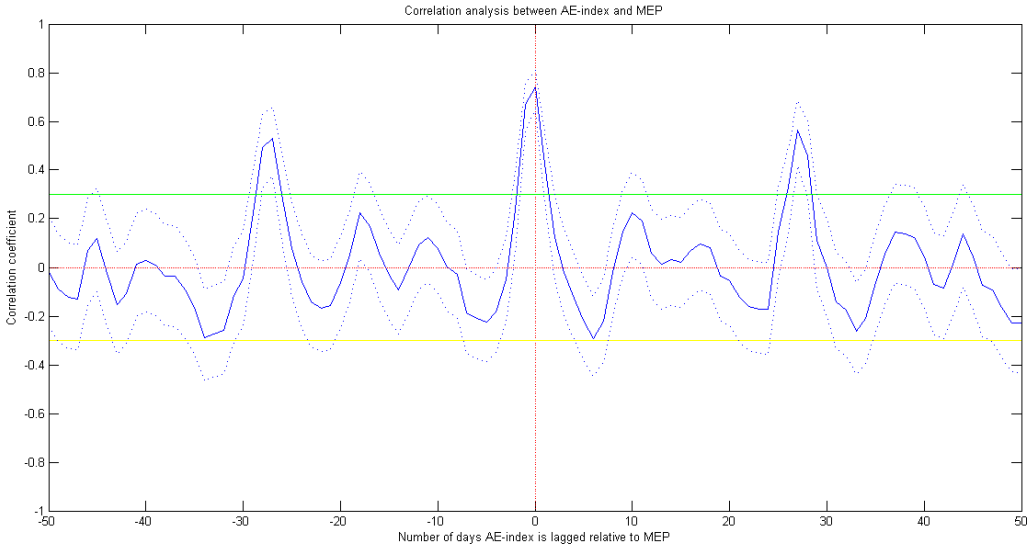

Figure 4.10: Cross-correlation analysis of the AE-index and MEP-values. The dotted lines represent the 95% confidence interval of the correlation coefficient. Positive lags translates to the MEP leading the AE-index. The green line indicates the threshold between weak and moderate correlations.

4.4.2 MEP-activity correlated with NO

Figure 4.11 displays the result of the cross-correlation between the MEP-activity and the NO-concentration. The r value after 5 day lag bordered close to the threshold of moderate correlation at 0.2705. Theoretical considerations dictate that any effect the MEP-activity would have on mesospheric NO production ought to occur within the same day of the precipitation. The observed 5 day delay is inconsistent with this. Medium energy precipitation is therefore not likely to be a significant source of NO in the middle atmosphere. A delay of 5 days does not fit with any known mechanism regarding precipitation induced NO synthesis.

Note the significant peaks at positive and negative lags of 27 days, both surpassing the threshold of 0.5 and indicating a moderate to good correlation. This periodicity is likely a result of the Sun's rotational period of 27 days, meaning areas of high and low activity are facing the Earth every 27 days.

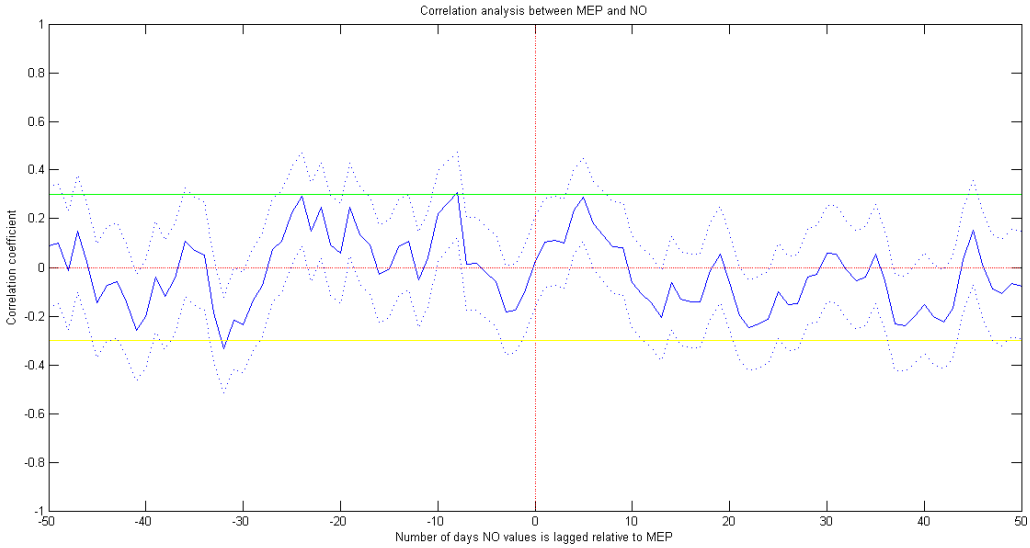

Figure 4.11: Cross-correlation analysis of NO-concentration and MEP-values. The dotted lines represent the 95% confidence interval of the correlation coefficient. Positive lags translates to the MEP leading the NO. The green line indicates the threshold between weak and moderate positive correlations.

4.4.3 24 hour tides correlated with NO

Figure 4.12 display the result of the cross-correlation between the 24 hour tide and the NO-concentration. The most significant correlation coefficients were observed to be at lags of 8 and 9 days, as listed in table 4.1. The 24 hour tidal amplitude accounts for 11.49 percent of the change in NO-concentration measured 9 days after the tide, and 9.57 percent 8 days after the tide. This is judged to be a moderate correlation as both correlation coefficients exceed 0.3. The 24 hour tidal component is therefore considered a plausible candidate for downward transport of nitric oxide into the mesosphere.

Lag (days)	Peak correlation coefficient	r value
8	0.3093	0.0957
9	0.3389	0.1149

Table 4.1: Table listing correlation coefficients, their r value and delay relative to the NO-data.

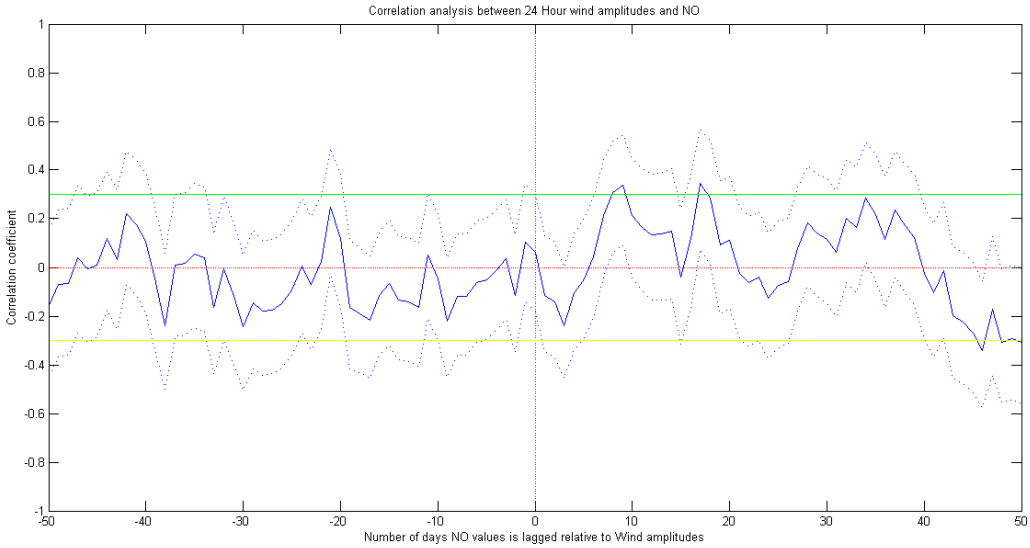

Figure 4.12: Cross-correlation analysis of NO-concentration and 24 hour tidal amplitudes. The dotted lines represent the 95% confidence interval of the correlation coefficient. Positive lags translates to the tide leading the NO. The green and yellow lines indicates the threshold between weak and moderate positive and negative correlations respectively.

4.4.4 12 hour tides correlated with NO

Figure 4.13 displays the result of the cross-correlation between the 12 hour tide and the NO-concentration. No positive correlation coefficients were observed before day 31. Negative correlation coefficients exceeding the threshold of moderate anti-correlation were observed after five days lag, peaking at -0.5104 after eight days of lag. This was close to the threshold of a strong anti-correlation, and the 95% confidence interval even passed the threshold of -0.6. This translates to less vertical transport of NO was occurring when the 12 hour tidal amplitude was low.

The 12 hour tidal component is therefore considered unlikely to be a significant source of downward transport of NO into the mesosphere.

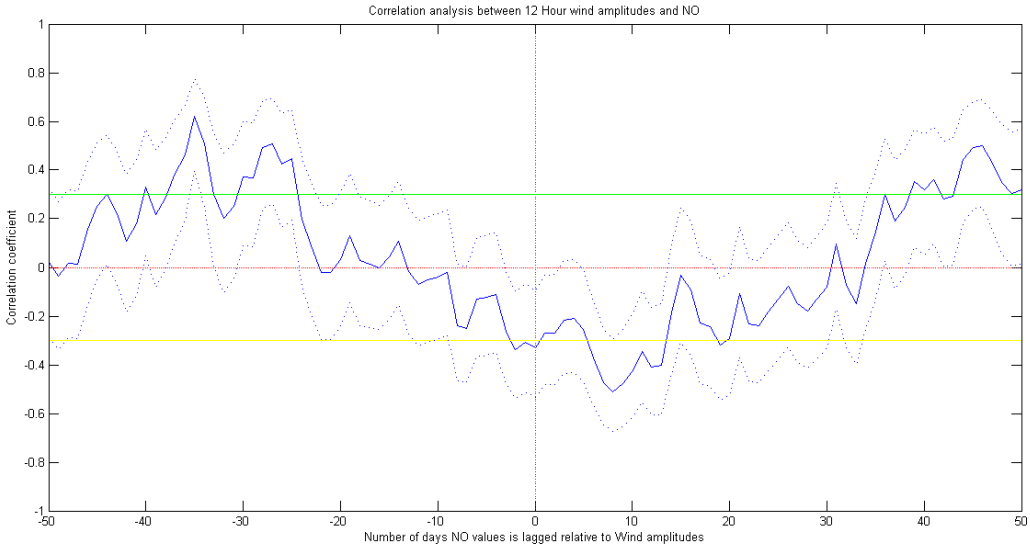

Figure 4.13: Cross-correlation analysis of NO-concentration and 12 hour tidal amplitudes. The dotted lines represent the 95% confidence interval of the correlation coefficient. Positive lags translates to the tide leading the NO. The green and yellow lines indicates the threshold between weak and moderate positive and negative correlations respectively.

4.4.5 Total tide correlated with NO

Figure 4.14 displays the result of the cross-correlation between the vector sum of the 12 and 24 hour tide and the NO-concentration. No positive correlations were observed within 33 days of positive lag. However, negative correlation coefficients exceeding the threshold of -0.3 were observed after between six and twelve days of lag, which indicated a moderate anti-correlation. This translates to more vertical transport occurring when the total tide was low.

The total tide is therefore considered unlikely to be a significant source of downward transport of NO into the mesosphere.

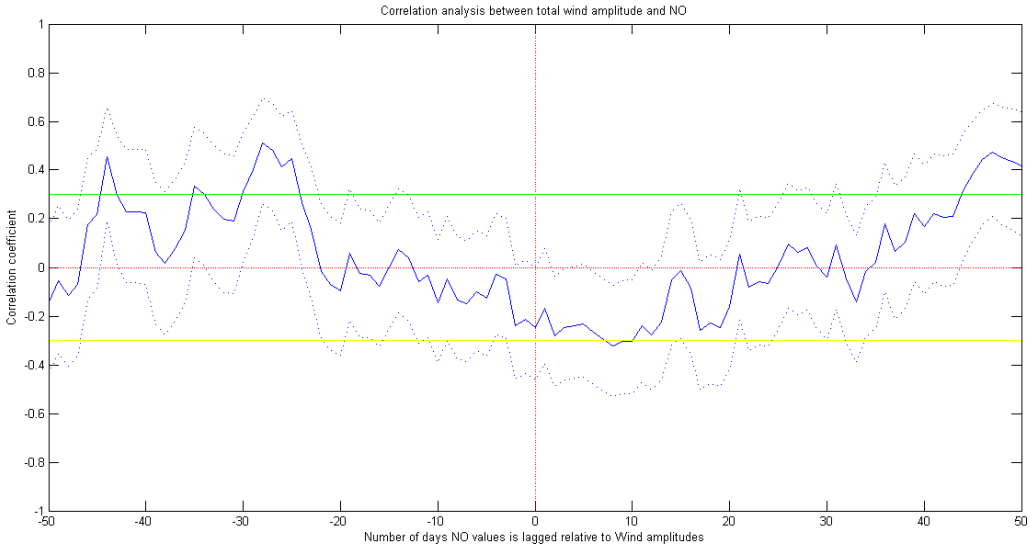

Figure 4.14: Cross-correlation analysis of NO-concentration and sum of 12 hour and 24 hour tidal amplitudes. The dotted lines represent the 95% confidence interval of the correlation coefficient. Positive lags translates to the tide leading the NO. The green and yellow lines indicates the threshold between weak and moderate positive and negative correlations respectively.

4.4.6 AE-modulated 24 hour tides correlated with NO

Figure 4.15 displays the result of the cross-correlation between the AE-modulated 24 hour tide and the NO-concentration. Table 4.2 lists the most prominent correlation coefficient value and lag. The correlation at five day lag displayed a profile reminiscent of the MEP and NO cross-correlation but were below the threshold of moderate correlation.

This suggests that the effects observed in the 24 hour wave not modulated by AE remained undisturbed, and the incidental correlation br

Lag (days)	Peak correlation coefficient	r value
8	0.3423	0.1172

Table 4.2: Table listing correlation coefficients, their r value and delay relative to the NO-data.

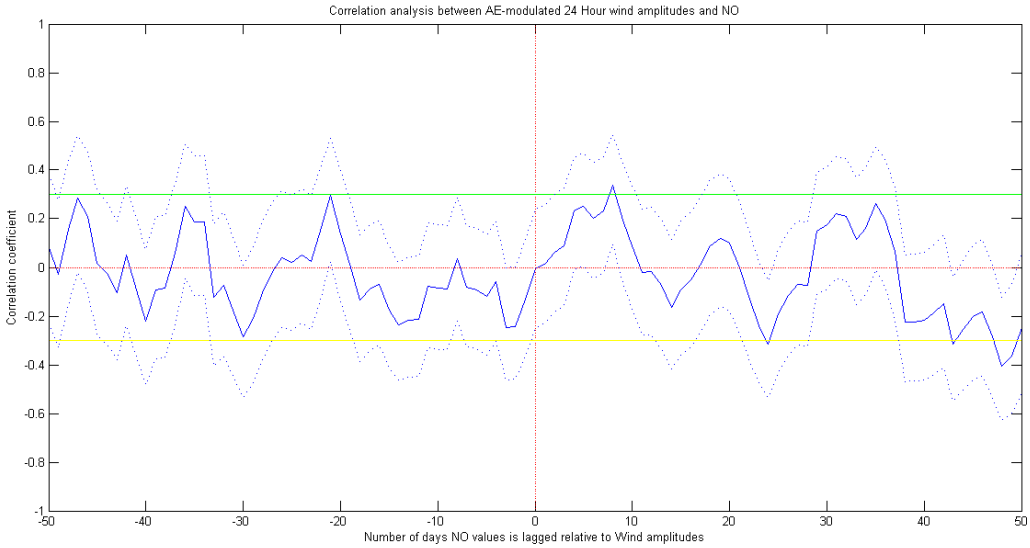

Figure 4.15: Cross-correlation analysis of NO-concentration and AE-modulated 24 hour tidal amplitudes. n and sum of 12 hour and 24 hour tidal amplitudes. The dotted lines represent the 95% confidence interval of the correlation coefficient. Positive lags translates to the AE-modulated tide leading the NO. The green and yellow lines indicates the threshold between weak and moderate positive and negative correlations respectively.

4.4.7 AE-modulated 12 hour tidal component correlated with NO

Figure 4.16 displays the result of the cross-correlation between the AE-modulated 12 hour tide and NO. All positively lagged correlation coefficients were consistently below 0.3, numbers which yielded low r-values. Only after a 17 day lag did moderate anti-correlation occur.

The AE-modulated 12 hour tidal component was judged unlikely to be the cause of downward transport of NO into the mesosphere.

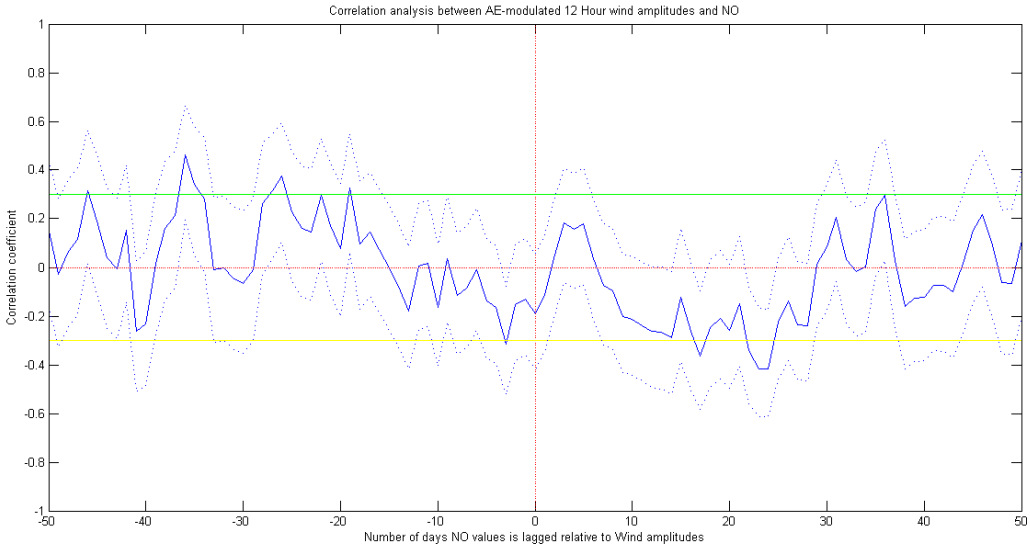

Figure 4.16: Cross-correlation analysis of NO-concentration and AE-modulated 12 hour tidal amplitudes. n and sum of 12 hour and 24 hour tidal amplitudes. The dotted lines represent the 95% confidence interval of the correlation coefficient. Positive lags translates to the AE-modulated tide leading the NO. The green and yellow lines indicates the threshold between weak and moderate positive and negative correlations respectively.

4.4.8 AE-modulated total tide correlated with NO

Figure 4.17 displays the result of the cross-correlation between the total tide and the NO-concentration. The positive correlation coefficients did not cross the threshold of moderate correlation, however a moderate anti-correlation was observed after 23 days.

Based on this the AE-modulated total wave was judged to be an unlikely candidate for downward transport of NO into the mesosphere.

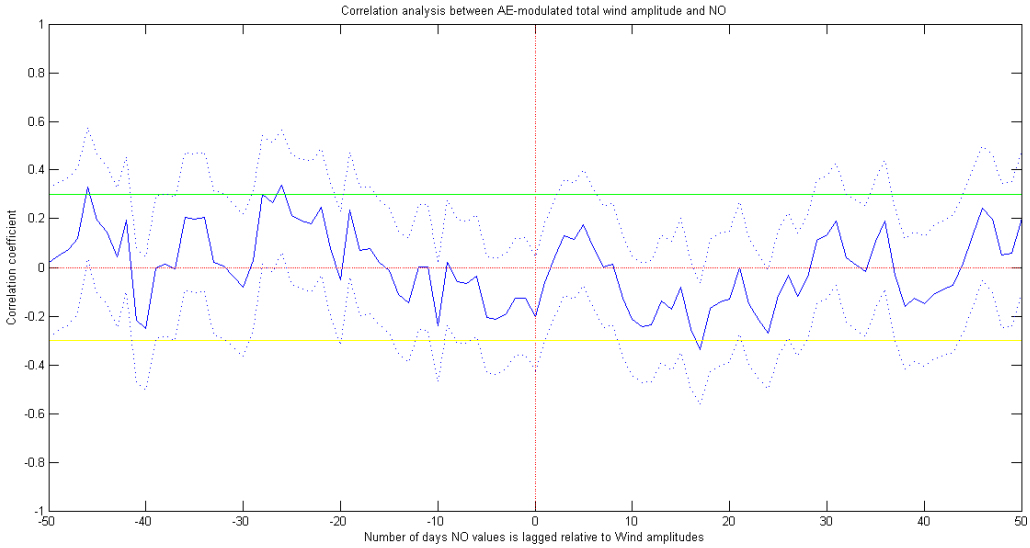

Figure 4.17: Cross-correlation analysis of NO-concentration and AE-modulated total tidal amplitudes. The dotted lines represent the 95% confidence interval of the correlation coefficient. Positive lags translates to the AE-modulated tide leading the NO. The green and yellow lines indicates the threshold between weak and moderate positive and negative correlations respectively.

4.4.9 AE-index correlated with NO

This correlation was performed in order to investigate the high correlation coefficients around day 5 of the AE-modulated data sets, and figure 4.18 displays the result. The AE-index correlated with NO yielded correlation coefficients somewhat similar to the MEP-values, which were deemed to be an unlikely source of NO-concentration in the mesosphere. After a delay of 5 days a correlation coefficient of 0.2705 was observed, closely resembling the results of the MEP-activity correlated with the NO. This translates to an r value of 0.0732, or that the AE-index accounted for 7.32 percent of the NO observed 5 days after the auroral electrojet activity occurred.

This implies that the increased correlation coefficients from around 5 days after the AE-modulated tides occurred were most likely connected to the correlation between the AE-index and the NO.

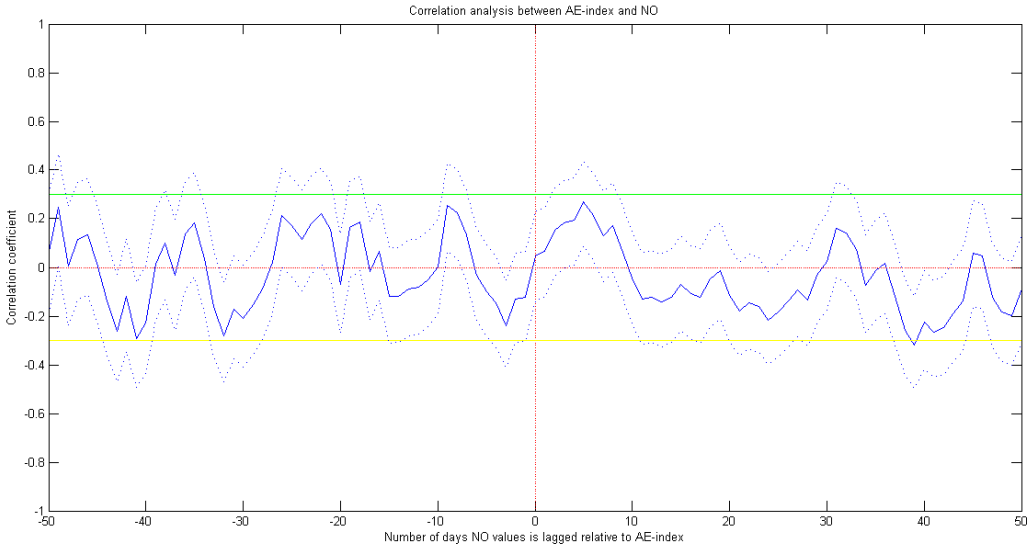

Figure 4.18: Cross-correlation analysis of NO-concentration and AE-values. The dotted lines represent the 95% confidence interval of the correlation coefficient. Positive lags translates to the AE-index leading the NO. The green and yellow lines indicates the threshold between weak and moderate positive and negative correlations respectively.

4.5 Delays

The energetic particle precipitation exhibits a notable four to five day delay when cross-correlated with the NO data, which is somewhat unexpected when compared to the theoretical framework. Due to the immediate nature of NO-synthesis from incoming energetic particles and photons, a delay of local production for several days after the precipitation has passed is unexpected. The correlation observed between the MEP-activity and NO is therefore likely to be incidental, although data sets spanning a longer time period would likely be able to give a more accurate answer to this question.

The wind data displayed a delay of up to nine days when correlated with the NO data. But this is less problematic due to the lifetime of NO at auroral latitudes being more than five days at altitudes over 90 kilometers, and increasingly longer further down. This means that large portions of the NO was likely to survive being transported downwards over such time periods.

4.6 The confidence intervals

It is important to note that the 95% confidence intervals represents the range of confidence coefficients which are 95% likely. This means that if the confidence intervals contained 0 or exceeded threshold values may not easily be ignored. The confidence intervals were also quite large, demon-

strating that the data displayed a notable uncertainty. This was most likely due to the rather short time span of overlapping data.

Chapter 5

Conclusion and future work

5.1 Local production of NO caused by MEP

This study did not find a significant correlation between precipitation activity and local production of NO in the mesosphere in 2008. The highest correlation coefficient, which did not surpass the threshold of being a moderate correlation, occurred after a lag of five days. This is inconsistent with the reaction speeds of NO synthesis and the instantaneous nature of energetic precipitation.

This may imply that some kind of transport was taking place within the span of five days after MEP activity, which was closely correlated with AE activity. Although the atmospheric tides did not seem to be the main cause of such a transport. The tides may even be impeding it.

5.2 Atmospheric tides as source of downward transport

The results from the cross-correlation performed on the Sanae wind data and the Troll NO data from 2008 hints at the 24 hour tidal component being connected to downward transport of nitric oxide into the middle atmosphere. The 24 hour component was calculated to account for 11.49 percent of the increased NO concentrations occurring with a lag of nine days. This level of correlation was judged to be significant.

However, the 24 hour component does not occur in isolation. The 12 hour component showed a moderate to strong anti-correlation with the NO, causing the total tide to yield low correlation coefficients as well. Because the total tide has the greatest effect on the atmosphere, due to opposite amplitudes canceling each other out. Another detail is that horizontal transport occurs at the same time as vertical transport, and horizontal transport towards lower latitudes would increase photo dissociation.

The mixed correlation and anti-correlation with the various tidal components points to tides are not affecting transport strongly and they may even have some detrimental effect.

5.3 Aurora-modulated atmospheric tides

This study did not find the aurora to have any significant effect on the atmospheric tides in terms of the correlation with the NO values. The slight increase in correlation coefficients after around five day delay was deemed to be a result of the correlation between the precipitation activity and the NO concentration. Only the 24 hour component displayed a moderate positive correlation after nine days. The 12 hour and total tide displayed moderate anti-correlations after more than 20 days, but otherwise remained inside the spectrum of low correlation.

This implied that the aurora had little or no effect on the ability of the atmospheric tides to transport NO.

5.4 Future work

The main challenge of this study was the limited time span of overlapping data, as short as 126 days, which limited the accuracy of the correlation analysis. If this subject is deemed to merit further study, a larger body of data spanning longer time periods would be key. This would minimize any coincidental fluctuations of the various data sets and grant more reliable correlation coefficients overall.

The effects of horizontal transport may also be interesting to examine, as increased photo dissociation from equatorward motion may also be influencing transport.

Bibliography

[1] Patrick J. Espy. Lecture slides: A microwave radiometer for the remote sensing of nitric oxide and ozone in the middle atmosphere, 2008.

[2] Patrick J. Espy. Lecture slides: Direct vs indirect no-production, 2016.

[3] David G. Andrews. *An introduction to Atmospheric Physics*. Cambridge University Press, 2010.

[4] R. E. Hibbins and M. J. Jarvis. A long-term comparison of wind and tide measurements in the upper mesosphere recorded with an imaging doppler interferometer and superdarn radar at halley, antarctica, 2008. ACP.

[5] E. Turunen. Lecture slides: Chemical effects of high-energy particle precipitation, 2007.

[6] Website of the world data center for geomagnetism, kyoto.

[7] Patrick J. Espy. Private communication, 2016.

[8] Hilde Nesse-Tyssoy. Private communication, 2016.

Appendix

5.5 Further correlations

5.5.1 The 8 hour tidal amplitude correlated with NO

Figure 5.1 displays the results of the cross-correlation between the 8 hour tidal amplitude component and the NO concentration. The correlation coefficients over the positive lags were consistently below 0.2, implying that this tidal amplitude does not have a significant effect on transport of NO.

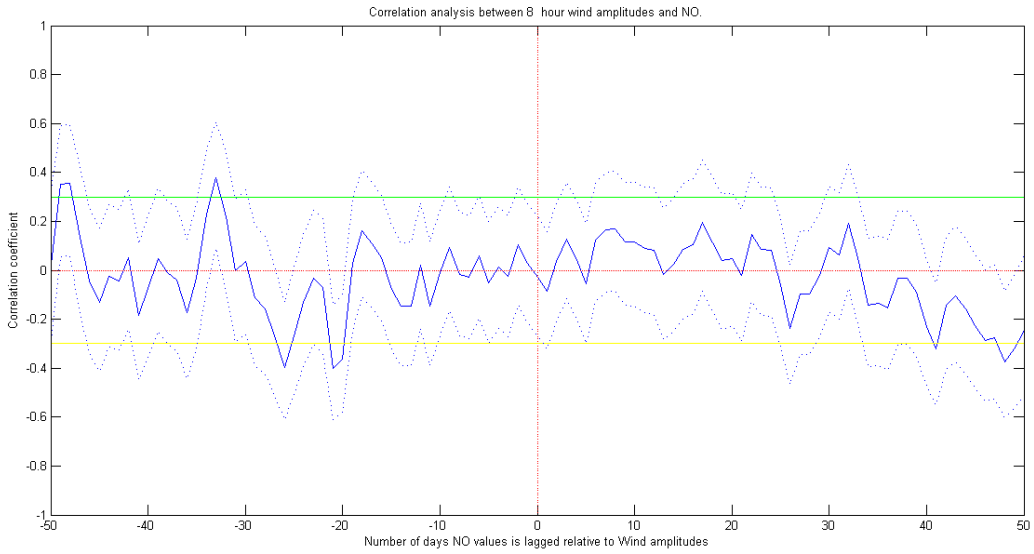

Figure 5.1: Cross-correlation analysis of NO-concentration and 24 hour tidal amplitudes. The dotted lines represent the 95% confidence interval of the correlation coefficient. Positive lags translates to the tide leading the NO. The green and yellow lines indicates the threshold between weak and moderate positive and negative correlations respectively.

5.5.2 The 48 hour tidal amplitude correlated with NO

Figure 5.2 displays the results of the cross-correlation between the 48 hour tidal amplitude component and the NO concentration. The correlation coefficient after 11 days lag equals 0.3601, giving an r-value of 0.1297. The coefficients observed at 6 and 7 days lag were also 0.3264 and 0.3078 respectively, giving r-values of 0.1065 and 0.0947. This hints to the 48 hour planetary wave being weakly correlated with downward transport of NO.

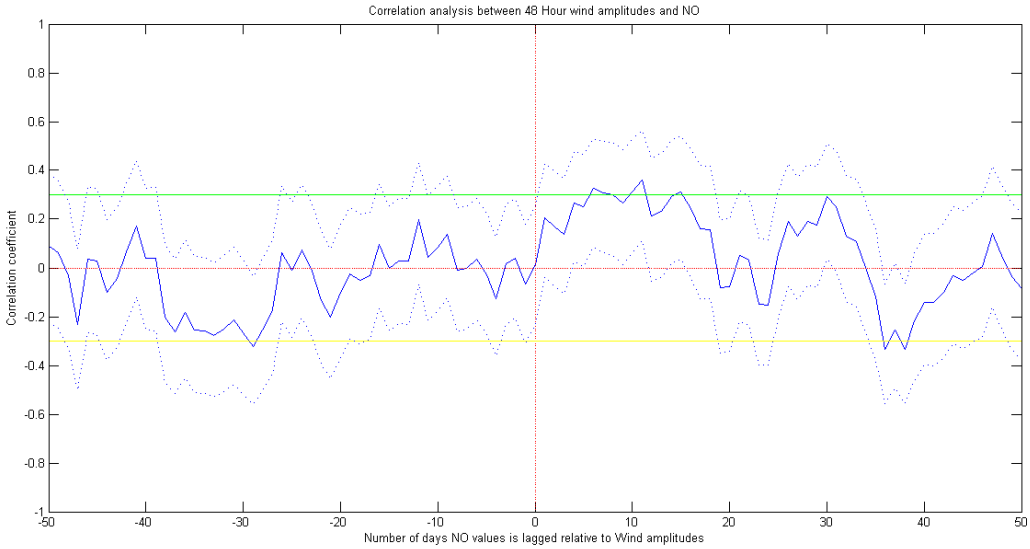

Figure 5.2: Cross-correlation analysis of NO-concentration and the 48 hour planetary wave. The dotted lines represent the 95% confidence interval of the correlation coefficient. Positive lags translates to the tide leading the NO. The green and yellow lines indicates the threshold between weak and moderate positive and negative correlations respectively.